Vol 18 No 9, September 2009
1674-1056/2009/18(09)/3909-09

Chinese Physics B

© 2009 Chin. Phys. Soc.
and IOP Publishing Ltd

The nonlinear propagation of acoustic waves in a viscoelastic medium containing cylindrical micropores*

Feng Yu-Lin(冯雨霖)[a], Liu Xiao-Zhou(刘晓宙)[a]†,
Liu Jie-Hui(刘杰惠)[a], and Ma Li(马 力)[b]

[a] *Key Laboratory of Modern Acoustics, Ministry of Education, Institute of Acoustics, Nanjing University, Nanjing* 210093, *China*

[b] *Institute of Acoustics, Chinese Academy of Sciences, Beijing* 100190, *China*

(Received 15 October 2008; revised manuscript received 16 February 2009)

Based on an equivalent medium approach, this paper presents a model describing the nonlinear propagation of acoustic waves in a viscoelastic medium containing cylindrical micropores. The influences of pores' nonlinear oscillations on sound attenuation, sound dispersion and an equivalent acoustic nonlinearity parameter are discussed. The calculated results show that the attenuation increases with an increasing volume fraction of micropores. The peak of sound velocity and attenuation occurs at the resonant frequency of the micropores while the peak of the equivalent acoustic nonlinearity parameter occurs at the half of the resonant frequency of the micropores. Furthermore, multiple scattering has been taken into account, which leads to a modification to the effective wave number in the equivalent medium approach. We find that these linear and nonlinear acoustic parameters need to be corrected when the volume fraction of micropores is larger than 0.1%.

Keywords: nonlinearity, cylindrical micropores, equivalent medium approach, multiple scattering
PACC: 4325, 4320

1. Introduction

Analytical theories of transmission phenomena are important to get the acoustic properties of materials which are used in modern underwater sound applications. Modeling the absorption of plane acoustic waves propagating in a viscoelastic medium is an important technical problem. Since the effects of acoustic absorption in a pure viscoelastic medium are not satisfactory, a medium with a porous structure is introduced to improve the attenuation. Several theoretical models are proposed to improve the attenuation. Oberst[1] and Meyer *et al*[2] introduced resonance by spherical perforations in the viscoelastic layers using a one-dimensional model. Gaunaurd[3] and Gaunand and Uberall[4] have extended the analysis to model the vibrations around one of the holes in the multi-perforated viscoelastic layer. Biot[5,6] considered the effect of frequency on the viscous forces within a porous medium and the kinematic viscosity was replaced by an oscillatory viscosity. His theory gave birth to a great number of theoretical works treating different geometries of propagation. In 1990, Ostrovsky[7] introduced a new porous 'rubber-like' medium, which has high attenuation of incident harmonic wave and strong acoustic nonlinearity. The finite element method was used to analyze harmonic wave propagation in viscoelastic gratings with pores in Refs.[8] and [9].

Most of the above work was based on the linear theory and some work has been done by using nonlinear methods.[10−12] The nonlinearity mentioned by Ostrovsky[7] was only at the low frequency area. The micropores oscillate vigorously at the frequency near the resonance range, thus behaving as a secondary source. Due to the nonlinear nature of the oscillation, high harmonics, particularly the second harmonic component become significant. Consequently, the nonlinearity of the host media is enhanced dramatically due to the presence of micropores. Fan *et al*[13] and Liang *et al*[14] have theoretically studied the nonlinear property of the viscoelastic medium containing spherical micropores by an approach based on an equivalent medium approach

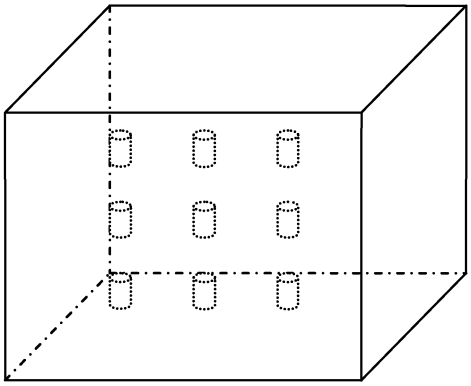
*Project supported by the National Natural Science Foundation of China (Grant No 10674066) and State Key Laboratory of Acoustics (Grant No 200802).

†Corresponding author. E-mail: xzliu@nju.edu.cn

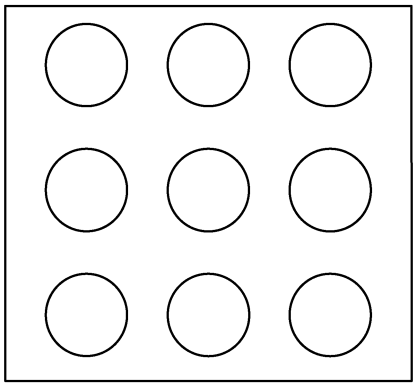
(EMA). They showed that such a medium can be highly nonlinear, even for a small density of pores per unit volume. Liang and Cheng[15] studied the acoustic localization in weakly compressible elastic media containing random spherical air bubbles. However, the synthesis of artificial nonlinear media with spherical pores poses a problem; cylindrical pores are far easier to fabricate. Ostrovsky[16] studied the nonlinear properties of an elastic medium with cylindrical pores at low frequency. The above study is based on EMA. However, it is shown that the classic theory of EMA using an ensemble average is a reduction of a complex system of scatterers and host medium to an 'effective medium'. A multiple scattering approach (MSA) was also used to study the nonlinear phenomena in porous media. The MSA looks at the mixture in a microscopic view and assumes that each bubble scatters waves which impinge on it. The wave pressure at any point of the bubbly liquid is the sum of the incident wave and the wave scattered by all the scatter bubbles. Foldy originated an MSA half a century ago.[17] Weston[18] and Miller[19,20] further developed it and named the scattering effect as the acoustic interaction of the gas bubbles. A lot of experiments and observations also got adequate explanations using this approach.[21,22] Several works have been developed to modify the classical theory by calculating the high order multiple scattering.[21−24] It is interesting to find that these modifications also progressed in two different ways, EMA[19] and MSA.[21,22]

In the present article, our model is supposed to be a rubberlike medium containing multiple cylindrical micropores (Fig.1), and investigates nonlinear acoustic wave propagation in such a medium at frequencies close to the resonant frequency of the micropores.

A one-dimensional model for a longitudinal wave through porous media with cylindrical pores is established. Combining the wave equation for the medium and the dynamic equation for cylindrical pores and using the perturbation method, we obtain equations for the fundamental and second harmonic wave. Then, by treating the medium containing micropores as a homogeneous medium, we can define the concept of the equivalent acoustic nonlinear parameter Γ. In this way, a formula to estimate the equivalent acoustic nonlinear parameter Γ of such media is achieved. The calculated results show that the sound field shows strong sound attenuation, dispersion and nonlinear properties. The multiple scattering effects on the sound velocity, attenuation and equivalent acoustic nonlinear parameter will also be discussed here. Both discussions will be demonstrated by several numerical examples, with some comparison between the two situations where the multiple scattering effects are considered or not. Finally we give the conclusions.



(a)



(b)

Fig.1. The model of a rubberlike medium containing multiple cylindrical micropores: (a) three dimensions; (b) two dimensions.

2. Theory

2.1. Longitudinal wave equation for a porous rubberlike medium

We consider a medium with microbubbles. If the amount of pores per wavelength is great enough, such a pore medium can be viewed as an equivalent continuous medium, and we can obtain the following equation:[13,24]

$$\frac{\partial^2\sigma_1}{\partial x^2}-\frac{1}{c_0^2(1+\mathrm{j}\eta)}\frac{\partial^2\sigma_1}{\partial t^2}=\rho N\frac{\partial^2 U_1}{\partial t^2},$$
$$\frac{\partial^2\sigma_2}{\partial x^2}-\frac{1}{c_0^2(1+\mathrm{j}\eta)}\frac{\partial^2\sigma_2}{\partial t^2}=\rho N\frac{\partial^2 U_2}{\partial t^2}. \qquad (1)$$

Here j is imaginary unit, σ means the x component of stress, U is defined as the volume fluctuation of

an individual bubble. $\eta = \dfrac{\eta_k K' + \dfrac{4}{3}\eta_M M'}{K' + \dfrac{4}{3}M'}$ refers to the viscosity of the pure medium, which is very small, $c_0 = \sqrt{\dfrac{K' + \dfrac{4}{3}M'}{\rho}}$ is the velocity of a longitudinal wave in the pure medium, ρ describes the density of the media and N is the number density of the micropores, K and M refer to the complex bulk modulus and the shear modulus of the medium, respectively, which can be expressed as

$$\begin{aligned} K &= K' + \mathrm{j}K'' = K'(1 + \mathrm{j}\eta_k), \\ M &= M' + \mathrm{j}M'' = M'(1 + \mathrm{j}\eta_M), \end{aligned} \tag{2}$$

where η_k and η_M are dissipation factors, and the 'averaged Hook' relating strain and stress for a longitudinal deformation can be written as [7]

$$\sigma = (\lambda + 2\mu)(\varepsilon - NU) = \left(K + \frac{4}{3}M\right)(\varepsilon - NU), \tag{3}$$

where λ, μ are Lame constants, ε is the x component of strain and we let

$$\sigma = \sigma_1 + \sigma_2 + \ldots, U = U_1 + U_2 + \ldots, \tag{4}$$

where σ_1, U_1 and σ_2, U_2 are the first-order and second-order terms, respectively.

2.2. Nonlinear wave equation for a cylindrical porous rubberlike medium

Considering the viscosity, we add the term $\gamma\dot{B}$ to the left of Eqs.(12) and (18) in Ref.[16], and the following equations can be obtained:

$$\frac{B_1\omega^2}{2}\ln\left(\frac{qr_0\omega}{2c_0}\right) + \frac{\mu B_1}{r_0^2\rho} - \frac{\mathrm{j}\pi\omega^2}{4}B_1 - \gamma\mathrm{j}\omega B_1 = \frac{\sigma_1}{\rho}, \tag{5}$$

$$\begin{aligned} &2\omega^2 B_2 \ln\left(\frac{qr_0\omega}{c_0}\right) + \frac{\mu}{\rho r_0^2}B_2 - \mathrm{j}\pi\omega^2 B_2 - \mathrm{j}2\omega\gamma B_2 \\ &= \frac{3}{2r_0^2}\left(\frac{\mu}{\rho r_0^2} - \frac{\omega^2}{4}\right)B_1^2 + \frac{\sigma_2}{\rho}, \end{aligned} \tag{6}$$

where $B = B_1 + B_2 + \ldots$, $B = R^2 - r^2 (U = \pi B l$, l is the length of the sample), r is the Lagrangian (initial) coordinate, R is its instantaneous coordinate, $S = \pi B$ is the variation of the area (or equivalently, the volume per unit length of the cylinder) in radial displacement of the particle, r_0 is the radius of the micropores, γ is the introduced parameter to describe the viscosity coefficient of the medium, $q = 1.78$.

Solving Eq.(5), we obtain

$$B_1 = \frac{\dfrac{\sigma_1}{\rho}}{\dfrac{\omega^2}{2}\ln\left(\dfrac{q\omega r_0}{2c_0}\right) + \dfrac{\mu}{r_0^2\rho} - \dfrac{\mathrm{j}\pi\omega^2}{4} - \gamma\mathrm{j}\omega}. \tag{7}$$

Substituting Eq.(7) into Eq.(6), we can obtain

$$\begin{aligned} B_2 = &\frac{\dfrac{\sigma_2}{\rho}}{2\omega^2\ln\left(\dfrac{qr_0\omega}{c_0}\right) + \dfrac{\mu}{r_0^2\rho} - \mathrm{j}\pi\omega^2 - \mathrm{j}2\omega\gamma} \\ &+ \frac{\dfrac{3}{2r_0^2}\left(\dfrac{\mu}{r_0^2\rho} - \dfrac{\omega^2}{4}\right)}{2\omega^2\ln\left(\dfrac{qr_0\omega}{c_0}\right) + \dfrac{\mu}{r_0^2\rho} - \mathrm{j}\pi\omega^2 - \mathrm{j}2\omega\gamma} \\ &\times \left(\frac{\dfrac{\sigma_1}{\rho}}{\dfrac{\omega^2}{2}\ln\left(\dfrac{qr_0\omega}{2c_0}\right) + \dfrac{\mu}{r_0^2\rho} - \dfrac{\mathrm{j}\pi\omega^2}{4} - \mathrm{j}\omega\gamma}\right)^2. \end{aligned} \tag{8}$$

Substituting Eqs.(7), (8) into Eq.(1), we can obtain the wave equations for fundamental and second harmonics as follows:

$$\begin{aligned} &\frac{\partial^2\sigma_1}{\partial x^2} - \frac{1}{c_0^2(1 + \mathrm{j}\eta)}\frac{\partial^2\sigma_1}{\partial t^2} \\ &= -\left[\frac{Nl\pi\sigma_1}{\dfrac{1}{2}\ln\left(\dfrac{q\omega r_0}{2c_0}\right) + \dfrac{1}{\omega^2}\dfrac{\mu}{r_0^2\rho} - \dfrac{\mathrm{j}\pi}{4} - \mathrm{j}\dfrac{\gamma}{\omega}}\right], \end{aligned} \tag{9}$$

$$\begin{aligned} &\frac{\partial^2\sigma_2}{\partial x^2} - \frac{1}{c_0^2(1 + \mathrm{j}\eta)}\frac{\partial^2\sigma_2}{\partial t^2} \\ &= -\frac{Nl\pi\sigma_2}{2\ln\left(\dfrac{qr_0\omega}{c_0}\right) + \dfrac{1}{\omega^2}\dfrac{\mu}{r_0^2\rho} - \mathrm{j}\pi - \mathrm{j}\dfrac{2\gamma}{\omega}} \\ &\quad - \rho Nl\pi D\sigma_1^2, \end{aligned} \tag{10}$$

where

$$\begin{aligned} D = &\left(\frac{\dfrac{3}{2r_0^2\rho^2}\left(\dfrac{\mu}{r_0^2\rho} - \dfrac{\omega^2}{4}\right)}{2\ln\left(\dfrac{qr_0\omega}{c_0}\right) + \dfrac{1}{\omega^2}\dfrac{\mu}{r_0^2\rho} - \mathrm{j}\pi - \mathrm{j}\dfrac{2\gamma}{\omega}}\right) \\ &\times \left(\frac{1}{\dfrac{\omega^2}{2}\ln\left(\dfrac{q\omega r_0}{2c_0}\right) + \dfrac{\mu}{r_0^2\rho} - \dfrac{\mathrm{j}\pi\omega^2}{4} - \mathrm{j}\gamma\omega}\right)^2. \end{aligned}$$

2.3. Fundamental frequency

To solve Eq.(9), we assume

$$\sigma_1 = \sigma_{1A}\exp[\mathrm{j}(\omega t - \bar{k}_1 x)],$$
$$\bar{k}_1^2 = A_1 - \mathrm{j}B_1. \tag{11}$$

Thus equation can be solved,

$$A_1 = \frac{k_0^2}{1+\eta^2} + Nl\pi\left[\frac{\frac{1}{2}\ln\left(\frac{q\omega r_0}{2c_0}\right) + \frac{1}{\omega^2}\frac{\mu}{r_0^2\rho}}{\left[\frac{1}{2}\ln\left(\frac{q\omega r_0}{2c_0}\right) + \frac{1}{\omega^2}\frac{\mu}{r_0^2\rho}\right]^2 + \left(\frac{\pi}{4} + \frac{\gamma}{\omega}\right)^2}\right], \tag{12}$$

$$B_1 = \frac{k_0^2\eta}{1+\eta^2} - Nl\pi\left[\frac{\frac{\pi}{4} + \frac{\gamma}{\omega}}{\left[\frac{1}{2}\ln\left(\frac{q\omega r_0}{2c_0}\right) + \frac{1}{\omega^2}\frac{\mu}{r_0^2\rho}\right]^2 + \left(\frac{\pi}{4} + \frac{\gamma}{\omega}\right)^2}\right], \tag{13}$$

where $k_0 = \dfrac{\omega}{c_0}$, $\bar{k}_1 = k_1 - \mathrm{j}\alpha_1$, $c_1 = \omega/k_1$, $\alpha_1 = \sqrt{\dfrac{\sqrt{A_1^2 + B_1^2} - A_1}{2}}$. Here c_1 means the dispersive sound velocity of the longitudinal wave and α_1 describes the attenuation coefficient of the fundamental frequency.

2.4. Second harmonic

Equation (10) is an inhomogeneous differential equation. The general solution of this kind of equation is the sum of the general solution of the associated homogeneous equation and of any particular solution. For the solution of the homogeneous equation, assuming

$$\sigma_2' = \sigma_{2A}'\exp[\mathrm{j}(2\omega t - \bar{k}_2 x)],$$
$$\bar{k}_2^2 = A_2 - \mathrm{j}B_2, \tag{14}$$

we can obtain

$$A_2 = \frac{4k_0^2}{(1+\eta^2)} + \frac{Nl\pi\left[2\ln\left(\frac{qr_0\omega}{c_0}\right) + \frac{1}{\omega^2}\frac{\mu}{r_0^2\rho}\right]}{\left[2\ln\left(\frac{qr_0\omega}{c_0}\right) + \frac{1}{\omega^2}\frac{\mu}{r_0^2\rho}\right]^2 + (\pi + \frac{2\gamma}{\omega})^2}, \tag{15}$$

$$B_2 = \frac{4k_0^2\eta}{(1+\eta^2)} - \frac{Nl\pi\left(\pi + \frac{2\gamma}{\omega}\right)}{\left[2\ln\left(\frac{qr_0\omega}{c_0}\right) + \frac{1}{\omega^2}\frac{\mu}{\rho r_0^2}\right]^2 + \left(\pi + \frac{2\gamma}{\omega}\right)^2}. \tag{16}$$

With the boundary condition: $x = 0$, $\sigma_2 = 0$, we finally obtain

$$\sigma_2 = \frac{\rho N\pi l D\sigma_{1A}^2}{4\bar{k}_1^2 - \bar{k}_2^2}[\exp(-\mathrm{j}\bar{k}_2 x) - \exp(-2\mathrm{j}\bar{k}_1 x)]\exp(2\mathrm{j}\omega t). \tag{17}$$

Like Refs.[13] and [24], we can introduce an equivalent acoustic nonlinear parameter for the second-harmonic generation

$$\Gamma = \frac{c_0^3\rho^2\pi NlD[\exp(-2\mathrm{j}\bar{k}_1 x) - \exp(-\mathrm{j}\bar{k}_2 x)]}{\omega x(4\bar{k}_1^2 - \bar{k}_2^2)}. \tag{18}$$

For a short propagation distance, the approximation $(\alpha_2 - 2\alpha_1)x \ll 1$, $(k_2 - 2k_1) \ll 1$ can be adopted to simplify the solution. Therefore the amplitude of the equivalent acoustic nonlinear parameter can be described as

$$\Gamma_{\mathrm{e}} = \frac{c_0^3\rho^2\pi NlD}{\omega\sqrt{(2k_1 + k_2)^2 + (2\alpha_1 + \alpha_2)^2}}. \tag{19}$$

2.5. Modified model considering multiple scattering

Considering the dissipation of the porous media, we can describe the propagation of the longitudinal wave as

$$\rho\frac{\partial^2\varepsilon}{\partial t^2}=\frac{\partial^2\sigma}{\partial x^2}+\eta\frac{\partial}{\partial t}\left(\frac{\partial^2\varepsilon}{\partial x^2}\right). \tag{20}$$

From Eq.(5), we can obtain

$$U=\frac{\sigma}{\rho}\pi l/\left[\frac{\omega^2}{2}\ln\left(\frac{qr_0\omega}{2c_0}\right)+\frac{\mu}{r_0^2\rho}-\frac{\mathrm{j}\pi\omega^2}{4}-\gamma\mathrm{j}\omega\right]. \tag{21}$$

Substituting Eq.(22) into Eq.(3), we can obtain the following equation:

$$\sigma=(\lambda+2\mu)\left\{\varepsilon-N\frac{\sigma}{\rho}\pi l/\left[\frac{\omega^2}{2}\ln\left(\frac{qr_0\omega}{2c_0}\right)+\frac{\mu}{r_0^2\rho}-\frac{\mathrm{j}\pi\omega^2}{4}-\gamma\mathrm{j}\omega\right]\right\}. \tag{22}$$

Supposing

$$A=\frac{\omega^2}{2}\ln\left(\frac{qr_0\omega}{2c_0}\right)+\frac{\mu}{r_0^2\rho}-\frac{\mathrm{j}\pi\omega^2}{4}-\gamma\mathrm{j}\omega. \tag{23}$$

we can write Eq.(20) as

$$\left[\frac{(\lambda+2\mu)\rho A}{\rho A+N\pi l(\lambda+2\mu)}+\eta(\mathrm{j}\omega)\right]\nabla^2\varepsilon+\rho\omega^2\varepsilon=0. \tag{24}$$

From Eq.(24), we can obtain

$$k^2=\frac{\rho\omega^2}{\dfrac{(\lambda+2\mu)\rho A}{\rho A+N\pi l(\lambda+2\mu)}+\eta(\mathrm{j}\omega)}. \tag{25}$$

As discussed before, η is very small and can be ignored here, then

$$k^2=k_0^2+\frac{2N\pi l\omega^2/\ln\left(\dfrac{qr_0k_0}{2}\right)}{\omega^2-\omega_0^2\ln\left(\dfrac{qr_0\omega_0}{2c_0}\right)/\ln\left(\dfrac{qr_0k_0}{2}\right)-2\mathrm{j}\left(\dfrac{\pi\omega^2}{4}+\gamma\omega\right)/\ln\left(\dfrac{qr_0k_0}{2}\right)}. \tag{26}$$

According to Kargl's correction[23] which considers the multiple scattering of micropores, we change all k_0 to k_m except the first k_0 on the right side. Then the above equation can be modified as follows:

$$k_m^2=k_0^2+\frac{2N\pi l\omega^2/\ln\left(\dfrac{qr_0k_m}{2}\right)}{\omega^2-\omega_0^2\ln\left(\dfrac{qr_0\omega_0}{2c_0}\right)/\ln\left(\dfrac{qr_0k_m}{2}\right)-2\mathrm{j}\left(\dfrac{\pi\omega^2}{4}+\gamma\omega\right)/\ln\left(\dfrac{qr_0k_m}{2}\right)}. \tag{27}$$

From the modified k_m, we can obtain the modified sound velocity and attenuation of the porous media; if we substitute k_1 in Eq.(19) with k_m, we can also obtain the modified equivalent acoustic nonlinear parameter. These linear and nonlinear sound parameters are corrected with multiple scattering.

3. Numerical results

We choose the material silicone for calculation, which shows representative rubberlike properties ($K/M\gg1$). The physical parameters of the material are listed in Table 1.

Table 1. Parameters of the silicone material.

material	silicone
density $\rho/(\mathrm{kg/m^3})$	1000
bulk modulus K/Pa	2.89×10^9
shear modulus M/Pa	4×10^5
K/M	7225
Young's modulus E/Pa	1.20×10^6
Poisson rate σ	0.49976

3.1. Phase velocity change with frequency

The sound velocity change with frequency at different radii of pores can be seen in Figure 2. The radius is respectively set to be 0.1 mm, 0.2 mm and 0.3 mm with the volume fraction of the pore NU=0.1%. The parameter η referring to the viscosity of the pure media can be ignored. The phase velocity is seen to decrease at very low frequencies and then increases rapidly until reaching its maximum in the vicinity of the resonant frequency. Beyond the resonant area, the influence of the pores vanishes and the phase velocity almost returns to the same value as the host medium. With the increase of the radius, the resonant frequency shifts lower and the sound velocity at the resonant frequency decreases. The change of the sound velocity and the right shift of its peak with increasing volume fraction are presented in Fig.3.

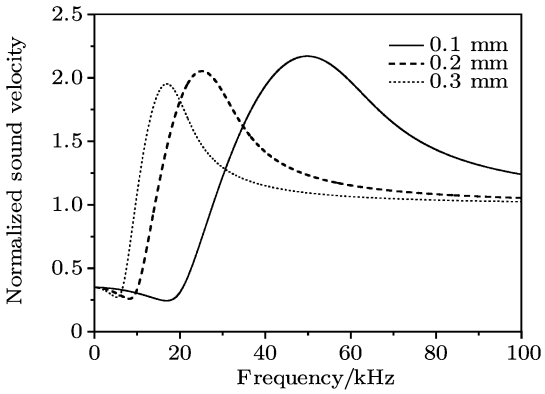


Fig.2. Normalized sound velocity change with frequency at different radii of pores (volume fraction is 0.1%), the solid curve represents radius 0.1 mm, the dashed curve represents radius 0.2 mm and the dotted curve represents radius 0.3 mm.

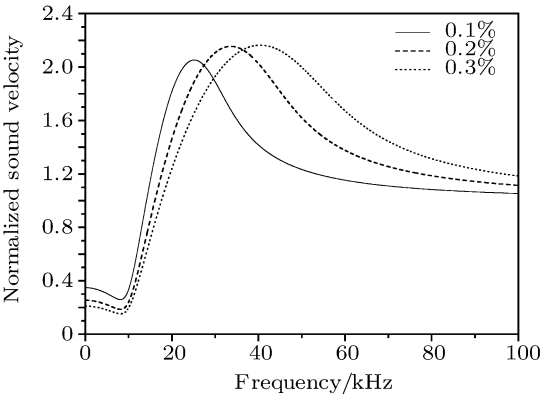


Fig.3. Normalized sound velocity change with frequency at different volume fractions of pores (radius is 0.2 mm), the solid curve represents volume fraction 0.1%, the dashed curve represents volume fraction 0.2% and the dotted curve represents volume fraction 0.3%.

3.2. Attenuation change with frequency

The attenuation change with frequency at different radii can be seen in Fig.4 with the same parameters as those in Fig.2. The attenuation is at a maximum near the resonant frequency of the pores because of the nonlinear oscillation of the pores. As a result, the coherent field is strongly attenuated. Beyond the resonant area, the attenuation shall gradually reach the same values as the no-pore media, as the micropores' effect can be negligible beyond the resonant frequency. With the increase of the radius, the peak position of the attenuation shifts to a lower frequency and the value decreases. This parameter of sound attenuation change with volume rate of pores can be seen in Fig.5. We can find that the attenuation increases with the increase of the volume rate of pores.

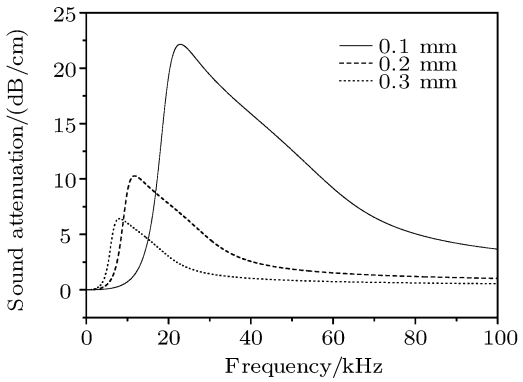


Fig.4. Sound attenuation change with frequency at different radii of pores (volume fraction is 0.1%), the solid curve represents radius 0.1 mm, the dashed line represents radius 0.2 mm and the dotted curve represents radius 0.3 mm.

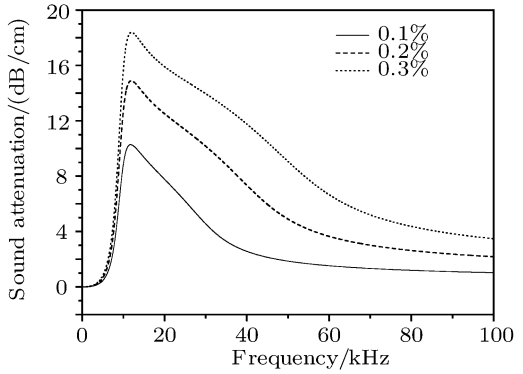


Fig.5. Sound attenuation change with frequency at different volume fractions of pores (radius is 0.2 mm), the solid curve represents volume fraction 0.1%, the dashed curve represents volume fraction 0.2% and the dotted curve represents volume fraction 0.3%.

3.3. Equivalent acoustic nonlinearity parameter

From Fig.6, it is found that the spectrum of the equivalent acoustic nonlinear parameter reaches its maximum at about the half of the resonant frequency of the micropores, which means that the mixture medium achieves the strongest nonlinearity around this frequency range (for example, when the radius of pore is 0.2 mm, the resonant frequency is 10 kHz, and the peak of the equivalent acoustic nonlinear parameter occurs near 5 kHz). Actually, the enhanced area also includes the range of resonant frequency of the pore. With the increase of radius, the equivalent acoustic nonlinear parameter decreases with its peak shifting to a lower frequency. Obviously, the equivalent acoustic nonlinear parameter increases when the volume fraction of the pores increases.

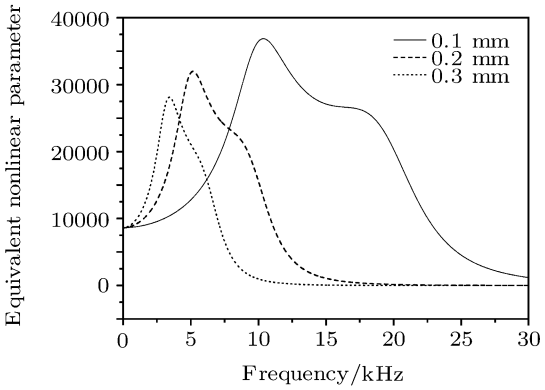


Fig.6. Equivalent nonlinear parameter change with frequency at different radii of pores (volume fraction is 0.1%), the solid curve represents radius 0.1 mm, the dashed curve represents radius 0.2 mm and the dotted curve represents radius 0.3 mm.

3.4. The effect of multiple scattering

When the volume fraction of pores is very small (NU=0.0001%), a comparison of sound velocity and attenuation between the correction of considering multiple scattering from Eq.(27) and the previous result from Eq.(26) indicates that the multiple scattering effect can be ignored, hence there is no difference between the no-correction curve and the correction curve (Figs.7 and 8). But the effect plays a negligible role when the volume fraction increases (Figs.9–12). The larger the volume fraction of the pore is, the greater the effect of the multiple scattering on the sound parameters is. The peak value increases remarkably due to the multiple scattering, which enhances the effects of these pores' nonlinear oscillations. Figure 13 shows the equivalent acoustic nonlinear parameter after taking multiple scattering into account. The increase of the equivalent acoustic nonlinear parameter after the correction means that the pore interaction will have a marked impact on the nonlinearity. Overall, the effect of multiple scattering does not act when the pores' volume fraction is very small or pores are sparsely arranged; however, the influence of pore interaction will gradually strengthen and then greatly enhance the sound parameters as the volume fraction of the pores grows.

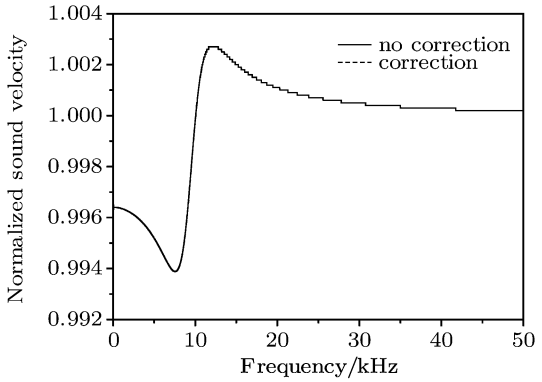


Fig.7. Normalized sound velocity based on the two models (the volume fraction is 0.0001%, radius is 0.2 mm): the solid curve represents no correction of multiple scattering, the dashed curve represents correction of multiple scattering.

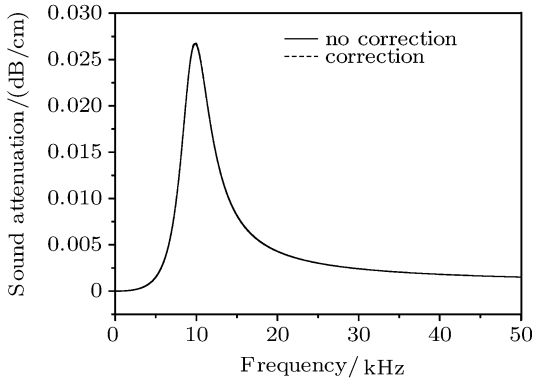


Fig.8. Sound attenuation based on the two models (the volume fraction is 0.0001%, radius is 0.2 mm): the solid curve represents no correction of multiple scattering; the dashed curve represents correction of multiple scattering.

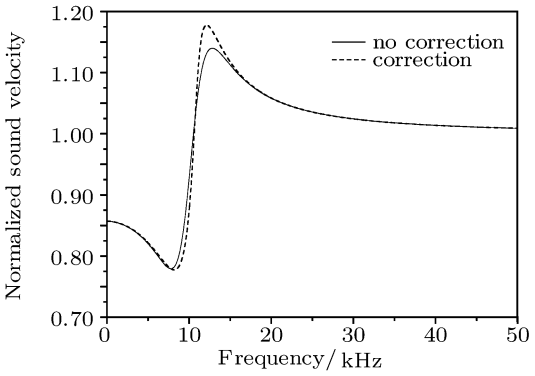


Fig.9. Normalized sound velocity based on the two models (the volume fraction is 0.005%, radius is 0.2 mm): the solid curve represents no correction of multiple scattering; the dashed curve represents correction of multiple scattering.

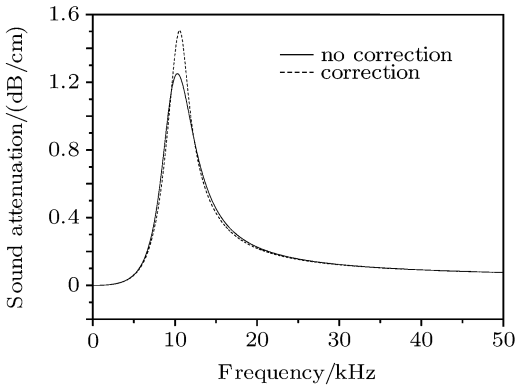


Fig.10. Sound attenuation based on the two models (the volume fraction is 0.005%, radius is 0.2 mm), the solid curve represents no correction of multiple scattering; the dashed curve represents correction of multiple scattering.

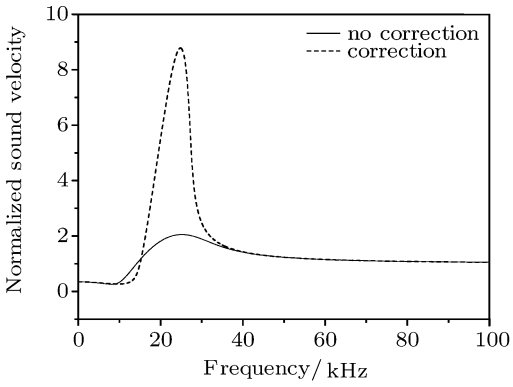


Fig.11. Normalized sound velocity based on the two models (the volume fraction is 0.1%, radius is 0.2 mm): the solid curve represents no correction of multiple scattering, the dashed curve represents correction of multiple scattering.

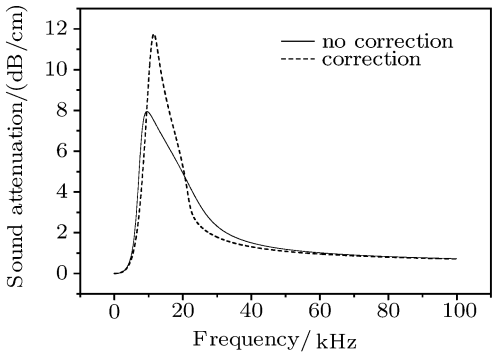


Fig.12. Sound attenuation based on the two models (the volume fraction is 0.1%, radius is 0.25 mm), the solid curve represents no correction of multiple scattering, the dashed curve represents correction of multiple scattering.

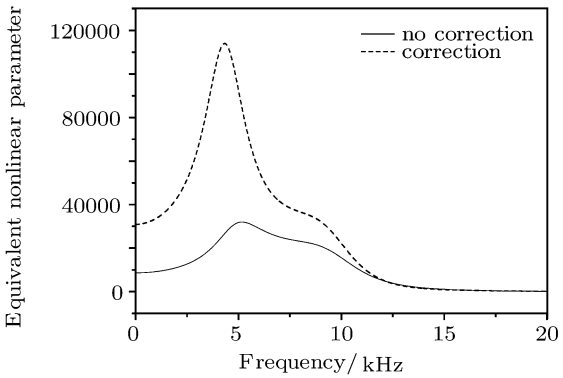


Fig.13. Equivalent nonlinear parameter based on the two models (the volume fraction is 0.1%, radius is 0.2 mm), the solid line represents no correction of multiple scattering, the dashed line represents correction of multiple scattering.

4. Comparison

As mentioned before, this kind of model of viscoelastic media containing sphere micropores has previously been investigated. Gaunaurd[3] did a cylindrical-style work, but his model had one difference from ours: his model cell has an inner radius 'a' and an outer one 'b', the inner rim is stress free and the outer is fixed. Our situation is an inner radius 'r_0' which is equal to 'a' but the outer is permitted to be infinity (because the size of the medium is much larger than that of r_0) and the boundary conditions are all stress free. Figure 14 shows his experimental results of measuring the absorption (or attenuation) coefficient at various frequencies when $a = 0.25$ mm (equal to our $r_0 = 0.25$ mm) and $b/a = 3$, which can be compared with Fig.12. The tendencies are nearly the same for the two models. The difference of the resonant frequency may come from the different model

details we have just discussed. Another parameter of volume fraction will only affect the value, not the tendency of the curves (shown in Fig.5).

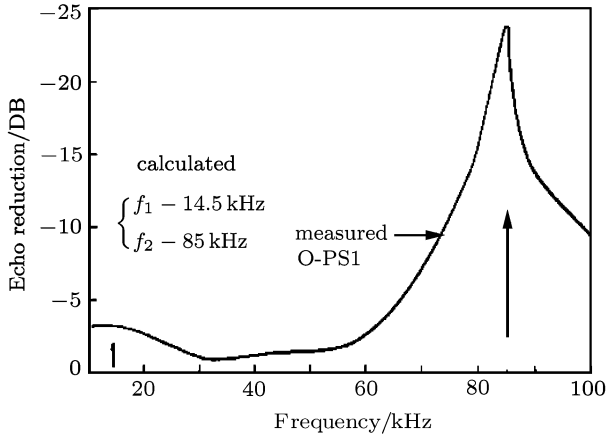


Fig.14. Gaunaurd's work (original figure is in Ref.[3], Fig.7).

5. Conclusion

In this paper, the sound velocity, sound attenuation and equivalent acoustic nonlinear parameter of a rubberlike medium containing cylindrical micropores have been studied theoretically. The results have revealed that when a viscoelastic medium contains cylindrical micropores, strong attenuation and strong dispersion are derived around the resonant frequency. Nonlinearity of the host medium at frequencies ranging around half of the resonant frequency of individual pores is greatly enhanced. An equivalent acoustic nonlinear parameter is defined to estimate the nonlinearity of the mixture medium. This model could be treated as a dilute mixture. When the volume fraction grows, multiple scattering among the pores is stronger and a modified model based on Kargl's correction is used to calculate the contributions to the parameters. The modification is necessary according to a comparison of the results of the theoretical calculation.

Acknowledgements

The authors thank Prof. Gong Xiufen and Prof. Zhu Zhemin for helpful discussions.

References

[1] Obsert H *Resonant Sound Absorbers* in: 1957 Richardon E G (editor) *Technical Aspects of Sound*
[2] Meyer E, Brendel K and Tamm K 1958 *J. Acoust. Soc. Am.* **30** 1116
[3] Gaunaurd G C 1977 *J. Acoust. Soc. Am.* **62** 298
[4] Gaunaurd G C and Uberall H 1978 *J. Acoust. Soc. Am.* **63** 1699
[5] Biot M A 1956 *J. Acoust. Soc. Am.* **28** 168
[6] Biot M A 1956 *J. Acoust. Soc. Am.* **28** 179
[7] Ostrovsky L A 1991 *J. Acoust. Soc. Am.* **90** 3332
[8] Hennion A C and Decarpigny J N 1991 *J. Acoust. Soc. Am.* **90** 3356
[9] Easwaran V and Munjal M L 1993 *J. Acoust. Soc. Am.* **93** 1308
[10] Qian Z W 1993 *Acta Phys. Sin.* **42** 949 (in Chinese)
[11] Quan Z W 1995 *Chin. Phys.* **4** 670
[12] Deng M X and Xiang Y X 2008 *Chin. Phys.* B **17** 4232
[13] Fan Z, Ma J, Liang B, Zhu Z M and Cheng J C 2006 *Acta Acustica United with Acustica* **92** 217
[14] Liang B, Zhu Z M and Cheng J C 2006 *Chin. Phys.* **15** 412
[15] Liang B and Cheng J C 2007 *Phys. Rev.* E **75** 016605
[16] Ostrovsky L A 1989 *Sov. Phys. Acoust.* **35** 286
[17] Foldy L L 1945 *Phys. Rev.* **67** 107
[18] Weston D E 1966 *J. Acoust. Soc. Am.* **39** 316
[19] Miller D L 1980 *Ultrasonics* **18** 277
[20] Miller D L 1981 *Ultrasonics* **19** 217
[21] Ye Z and Ding L 1995 *J. Acoust. Soc. Am.* **98** 1629
[22] Henyey F S 1999 *J. Acoust. Soc. Am.* **105** 2149
[23] Kargl S G 2002 *J. Acoust. Soc. Am.* **111** 168
[24] Ma J, Yu J F, Fan Z, Zhu Z M, Gong X F and Du G H 2004 *J. Acoust. Soc. Am.* **116** 186